Supporting Material

Mechanism of Membrane Permeation Induced by Synthetic β-Hairpin Peptides

Kshitij Gupta,[1] Hyunbum Jang,[2] Kevin Harlen,[3] Anu Puri,[1] Ruth Nussinov,[2] Joel Schneider,[3] and Robert Blumenthal[1,*]

[1] Basic Research Laboratory, Center for Cancer Research, [2]Basic Science Program, SAIC-Frederick, Inc., [3]Peptide Design and Materials Section, Chemical Biology Laboratory, National Cancer Institute, National Institutes of Health, Frederick, MD 21702 U.S.A.

***Corresponding author:** Robert Blumenthal, Center for Cancer Research, National Cancer Institute, PO Box B, Building 469, Room 246A, Frederick, MD 21702, Tel: 301-846-5532; Fax: 301-846-5598, E-mail: blumenthalr@mail.nih.gov

Keywords: antimicrobial peptides, liposomes, membrane bilayer, phosphatidylserine, molecular dynamics, Tb/DPA, calcein, membrane pore size, fluorescent dextran, β-hairpin peptides

Running title: Membrane permeation induced by synthetic β-hairpin peptides

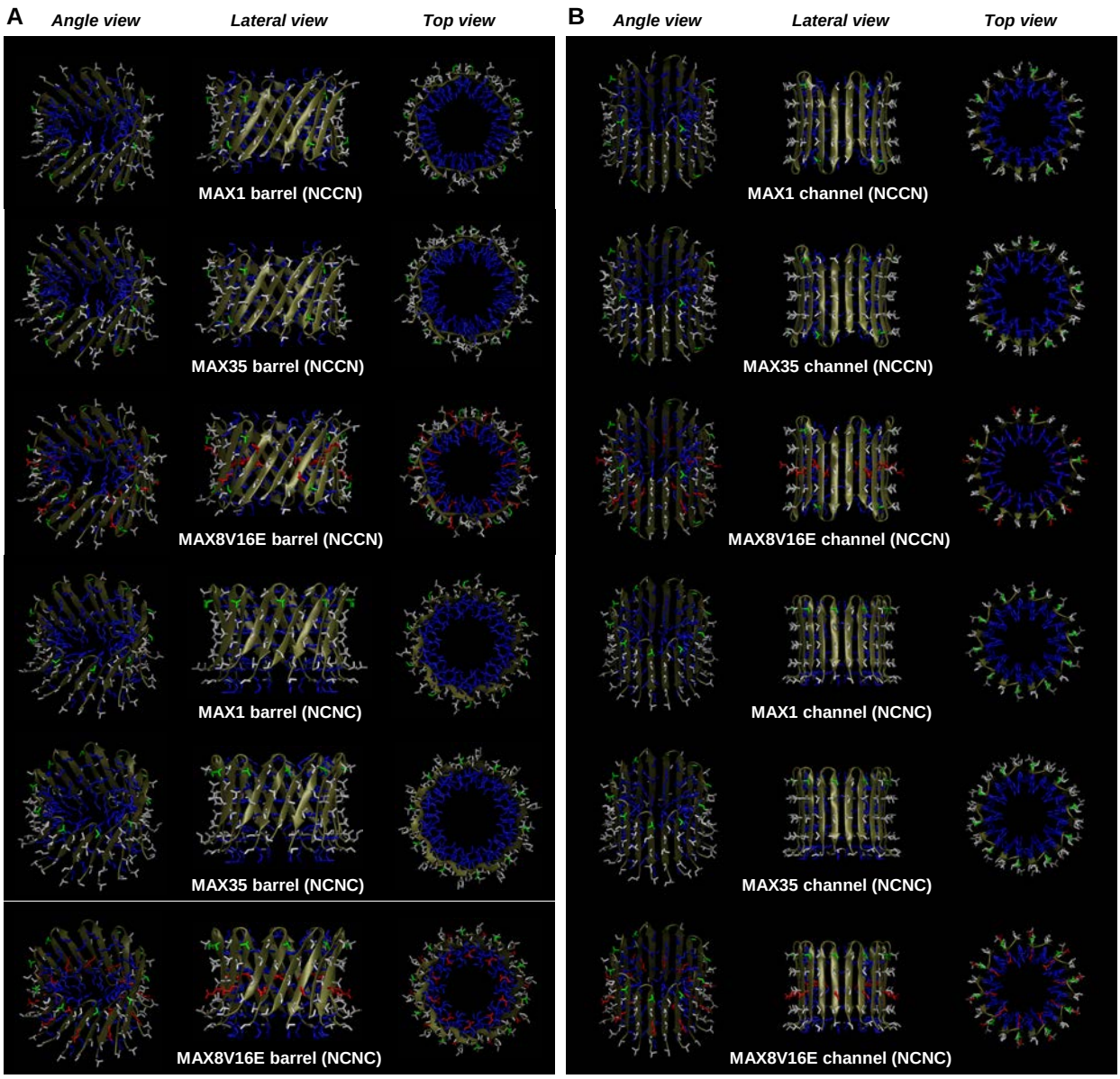

FIGURE S1 Conceptual designs of annular antiparallel β-sheet structures in a cartoon representation for the 10-mer MAX (A) barrels and (B) channels in the NCCN and NCNC packing modes. In the peptides, positively charged Lys side-chain is shown in blue, hydrophobic Val and Ile side-chains are shown in white, polar Thr side-chain is shown in green, and negatively charged Glu side-chain is shown in red (MAX8V16E barrel/channel only).

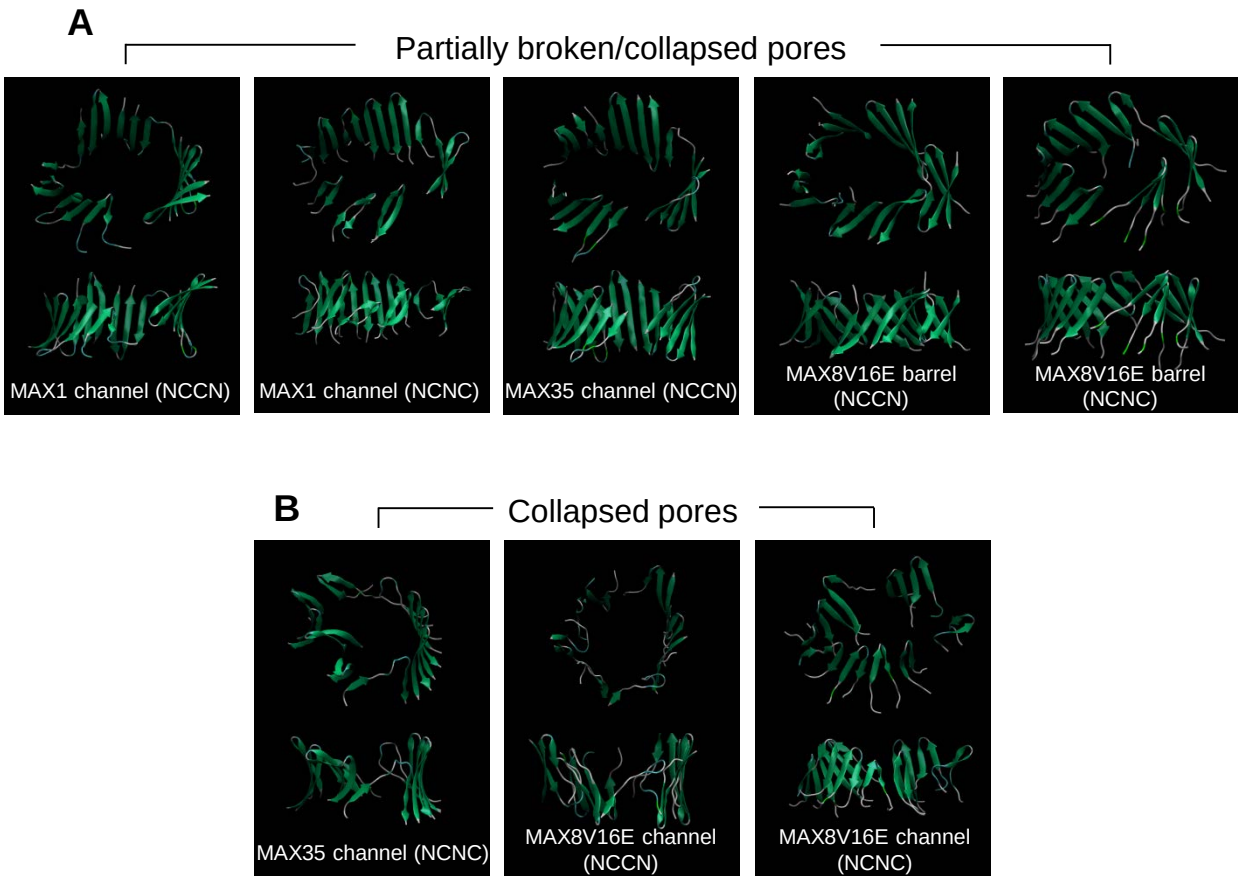

FIGURE S2 Averaged barrel/channel structures in the ribbon representation for the MAX1 and MAX35 channels, and MAX8V16E barrels/channels in the NCCN and NCNC packing modes with the (A) partially broken/collapsed and (B) collapsed pores during the simulations.

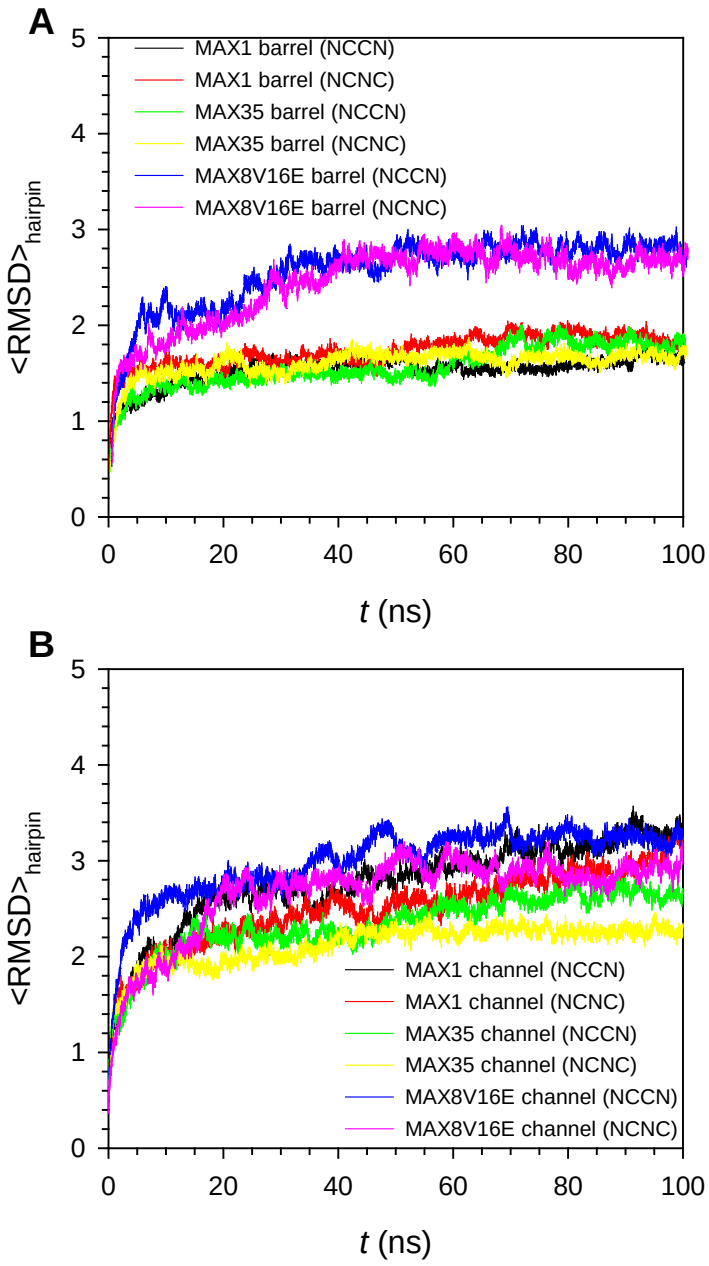

FIGURE S3 Time series of hairpin averaged root-mean-squared deviation, $\langle RMSD \rangle_{hairpin}$, from the starting point for C_α atoms of the peptides for the MAX (A) barrels and (B) channels in the NCCN and NCNC packing modes.

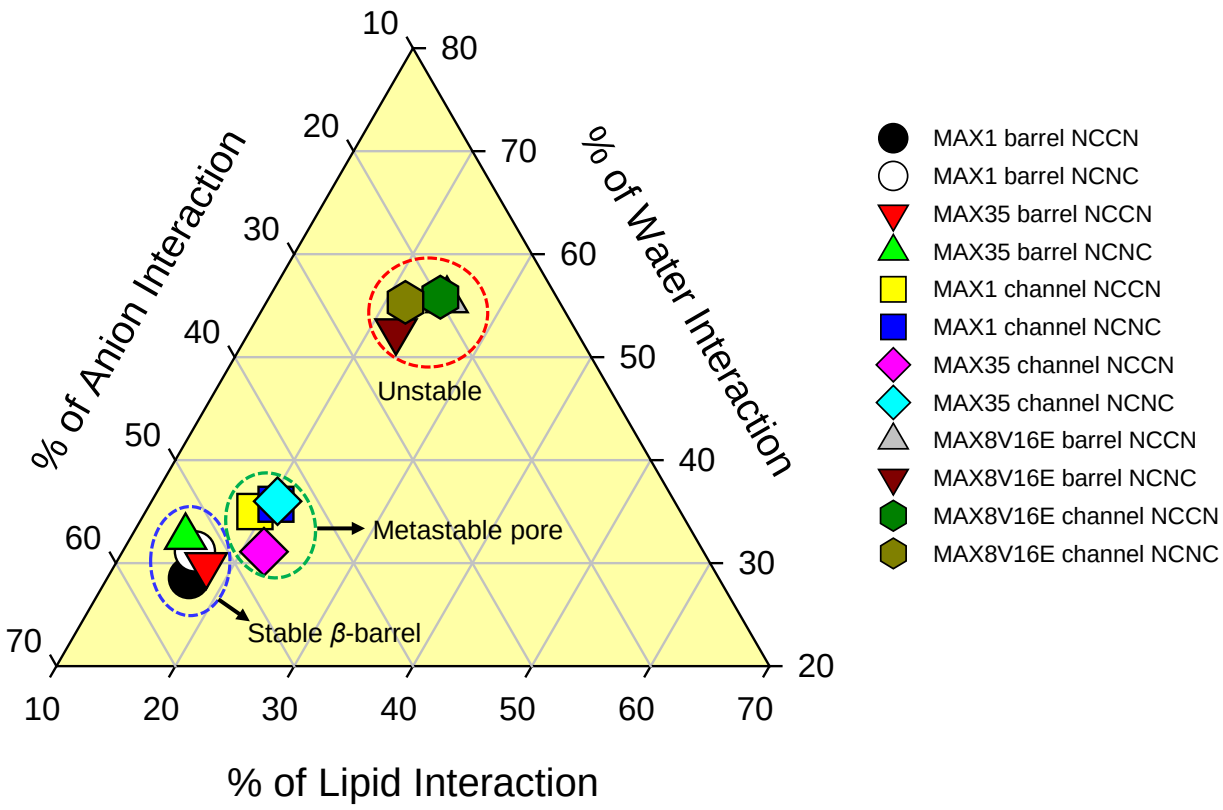

FIGURE S4 The percentage of peptide-solvent interactions for three components, lipid, water, and anion (Cl^-). The interaction energies of each MAX β-hairpin with lipids, waters, and anions are calculated, and then averaged over the time and the number of peptide in the barrel/channel.

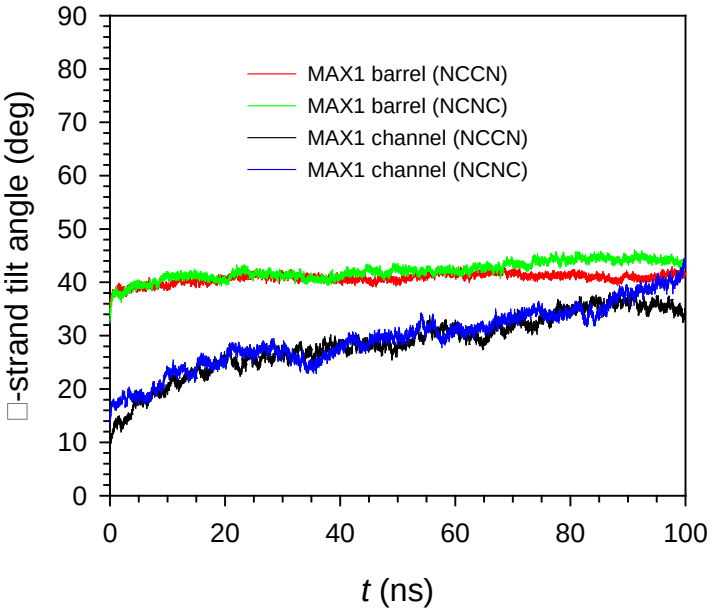

FIGURE S5 Time series of β-strand tilt angle with respect to the membrane normal for the MAX1 barrels/channels in the NCCN and NCNC packing modes.

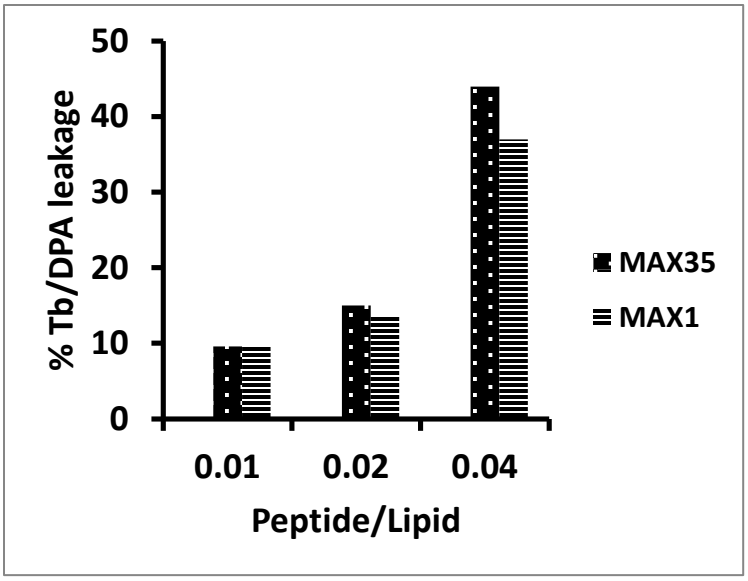

FIGURE S6 MAX35 and MAX1 induced Tb/DPA leakage from POPC/POPG (1:1) liposomes.

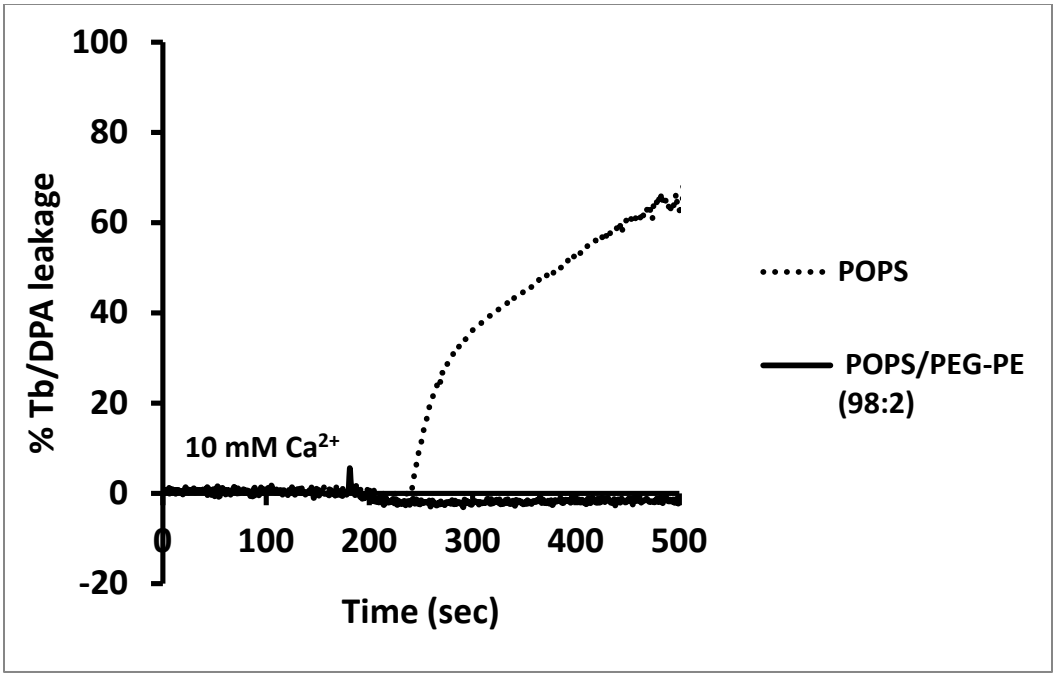

FIGURE S7 Inclusion of 2 mole% PEG-PE in POPS liposomes inhibited Ca^{2+} induced leakage.

DOCUMENT S1

Liposome preparation

Liposomes of POPC/POPS or POPC/POPS/PEG-PE - of different mole ratios were prepared either by probe sonication or by reverse phase evaporation (REV) methods (1). We used the following molecules for entrapment into liposomes: Tb/DPA, calcein, inulin, and TRD-40k. Exact lipid ratios and the type of molecules entrapped in the liposomes for various experiments are described in the corresponding figure legends. For Tb/DPA, calcein or inulin entrapment, sonicated liposomes were prepared. For entrapment of TRD-40k, liposomes were formed by reverse phase evaporation as described below.

Sonicated liposomes–Lipids dissolved in $CHCl_3$ were mixed at desired molar ratios in a glass tube and a lipid film was formed by removing $CHCl_3$ under nitrogen at room temperature. Any residual $CHCl_3$ was removed by placing the films overnight in a vacuum desiccator.

After hydrating the lipid films using the above mentioned solutions, samples were mixed by vigorous vortexing to generate multilamellar liposomes. Multilamellar liposomes were sonicated at 4°C by using a Probe Sonicator (Branson Ultrasonics (Shanghai) Co., Ltd, China). Typically, 10 minutes of sonication (1-minute pulses and 1-minute rest) yielded unilamellar liposomes ~100 nm in diameter, as determined by Zeta Nanosizer (see below). The sonicated liposomes were centrifuged at 1,500 × g for 5–10 minutes to remove any titanium particles and larger aggregates. Un-encapsulated solutes were removed from liposome-entrapped molecules as follows: Tb/DPA loaded liposomes (2) were separated from non-entrapped Tb/DPA, using a size-exclusion gel chromatography column (Sephadex G-50, 40 cm × 1 cm), pre-equilibrated with buffer 1. Liposome-encapsulated Tb/DPA was analyzed by measuring fluorescence at λ_{ex} = 276 and λ_{em} = 545 nm (see below Tb/DPA leakage assay). Calcein (mw. ~ 622.55; R_h ~ 0.74 nm) loaded liposomes to determine graded versus all or none mechanism were fractionated on a Sepharose CL-6B column (40 cm × 1 cm) pre-equilibrated with buffer 1. 1 mL fractions were collected and liposome-entrapped calcein was assayed by fluorescence measurements at λ_{ex} = 490 and λ_{em} =517 nm. For Inulin (mw. ~ 5000; R_h ~ 1.39 nm) loaded liposomes, 50 µCi ^{3}H-inulin was added to the lipid mixture. Inulin loaded liposomes were eluted through Sepharose CL-6B column pre-equilibrated with buffer 1 (pH 6.6). 1 mL fractions were collected and 0.1 mL from each fraction was analyzed for ^{3}H-inulin using 10 mL of scintillation fluid (ECOscint A, National Diagnostics, Atlanta, GA) in a scintillation counter (LS6500 Multi–purpose Scintillation counter, Beckman Coulter™, Brea, CA).

Reverse phase evaporation vesicles–Texas red dextran 40,000 (TRD-40k, mw. ~ 40,000; R_h ~ 5 nm) and calcein (mw. ~ 622.55; R_h ~ 0.74 nm) were co-encapsulated in POPC/POPS/PEG-PE (1:1:0.02 mole ratio) liposomes to study their simultaneous release (3). Liposomes were prepared by Reverse-phase evaporation method for maximal encapsulation of TRD-40k and calcein (4). Briefly, the lipid mixture for each composition was dried under high vacuum (10 mmHg) in a rotary evaporator (Heidolph, Elk Grove Village, IL) to obtain a lipid film with no residual chloroform. The lipid film was then dissolved in 1 mL of diethyl ether. 0.34 mL of TRD-40k (100 µM) and calcein (5 mM), dissolved in aqueous solution (buffer 1), was added and the mixture was sonicated in a bath-type sonicator for 5 min or longer until a stable emulsion was obtained. Ether was removed gradually in a rotary evaporator at room temperature under low vacuum (360-560 mmHg). The resulting gel was then disrupted by vortex mixing 2-3 times and the ether was further evaporated under higher vacuum (160-260 mmHg) until an opalescent aqueous suspension was obtained. An additional 0.66 mL of the aqueous solution of

TRD-40k and calcein was added. Any residual ether was further evaporated under high vacuum (10 mmHg) for 20 min. Resulting liposomes were analyzed for size by Malvern Zetasizer Nano ZS instrument as described above. The liposomes were then passed through a Sepharose CL-6B column pre-equilibrated with buffer 1 to remove any un-encapsulated TRD-40k and calcein. Liposome-rich fractions loaded with mentioned aqueous markers, obtained by gel permeation chromatography above were pooled together and were analyzed for their size and/or charge. The total phospholipid content was determined by inorganic phosphate analysis (5).

Size and Zeta potential measurements

A Malvern Zetasizer Nano ZS instrument (Southborough, MA) with a back-scattering detector was used to measure the hydrodynamic size (i.e., diameter) of liposomal formulations with and without addition of MAX peptides at L/P = 24 in batch mode (i.e., no fractionation) at 25°C in a disposable sizing/zeta cuvette. All the samples were in buffer 2 with 0.1 mM EDTA (final concentration) buffer at pH 7.4. The Stokes-Einstein equation was used to measure the hydrodynamic size of the liposomes and the Smoluchowski approximation was used to calculate Zeta potential from the electrophoretic mobility (6). The data are represented as "mean ± standard deviation" of triplicate samples from two independent experiments. Size and Zeta potential of liposomes + peptide were compared with liposomes without peptide and analyzed by the Holm-Sidak method using the ANOVA (Sigmaplot, Systat Software, Inc., San Jose, CA).

Circular dichroism studies

CD spectra were collected on an Aviv model 420 Circular Dichroism Spectrometer (AVIV Biomedical, Lakewood, NJ). Wavelength scans were recorded using a 1 nm step size and a 2 second averaging time at 5°C with a 5-minute equilibration time. Spectra were collected using a 1 mm quartz cell. All peptide, liposome, buffer and water samples were kept on ice prior to recording the spectra. Spectra were recorded in buffer 2 with or without 0.1 mM EDTA. To prepare samples an initial stock of peptide was diluted to twice the desired concentration in water. This stock was then diluted 1:1 with a 2× buffer 2 giving the desired sample and buffer concentrations. The sample was then immediately added to a liposome solution and the entire sample mixture was then added to the CD cell. For samples not including liposome the peptide in the desired buffer concentrations was added directly to the CD cell. Concentrations and volumes of buffer, peptide and liposome added to the CD cell varied depending on the desired lipid: peptide ratio and the initial concentrations of peptide and liposome solutions. Mean residue ellipticity (θ) was calculated using the following equation: $\theta = (\theta obs - \theta blank) / [(10)(l)(C)(r)(1000)]$ where θ blank is the ellipticity of either the buffer or liposome solution without peptide present, *l* is the path length of the cell (cm), C is the peptide concentration (M) and *r* is the number of residues.

Solute release assays

Tb/DPA leakage assay–The assay (7,8) was performed in a Fluorimeter (Fluoromax-3, Horiba Jobin Yvon, Edison, NJ) equipped with a water bath maintained at 25°C. The samples were placed in a quartz cuvette under constant stirring at a final concentration of 0.1 mM EDTA in buffer 2. The initial fluorescence of Tb/DPA (λ_{ex} = 276 nm and λ_{em}= 545 nm) in the liposomes was set to 100% value. Peptide-induced leakage of liposome entrapped Tb/DPA was determined by a decrease in fluorescence intensity due to the quenching of the Tb^{3+} by EDTA present in the external buffer. Octyl-*β*-D-glucopyranoside (OG) at 1% w/v final concentrations was used to

obtain maximum leakage (100%) that corresponds to minimum fluorescence. The extent of release, R(t), calculated by using the formula $R(t) = 100 \times [I(0) - I(t)]/[I(0) - I(f)]$, where I(0) is the initial fluorescence of the Tb/DPA liposomes before addition of membrane-active agents, I(t) is the fluorescence intensity at time t after addition of membrane-active agents, and I(f) is the fluorescence obtained when all the liposome contents leak that corresponds to maximum leakage caused by OG. The data in Figure 4B were fitted to a Langmuir isotherm $f=a*x/(b+x)$, where *f* is extent of release, *a* represents maximal release, and *b* is the concentration of peptide at half-maximal release using Sigmaplot (Systat Software, Inc., San Jose, CA).

Inulin release assay–Liposomes of POPC/POPS/PEG-PE (1:1:0.02, mole ratio) loaded with inulin were treated with MAX1 at L/P =24 and then re-fractionated as above. Untreated (control) liposomes were also fractionated under identical conditions. Release of ^{3}H-inulin was measured using 10 mL of scintillation fluid (ECOscint A, National Diagnostics, Atlanta, GA) in a scintillation counter (LS6500 Multi–purpose Scintillation counter, Beckman Coulter^{TM}, Indianapolis, IN).

Calcein release assay–Calcein release assay was performed to determine the graded versus all-or-none leakage mechanisms from liposomes upon interaction with peptides (9). POPC/POPS/PEG-PE (1:1:0.02 mole ratio) liposomes were loaded with 4, 10, 25, 50 or 100 mM calcein in buffer 1.The quenching ratio (Q) in each liposome preparation was determined by measuring fluorescence at λ_{ex}= 490 nm and λ_{em} = 517 nm using the Fluoromax-3 fluorimeter (Horiba Jobin Yvon, Edison, NJ) before and after adding 1% OG. Liposomes were then treated with MAX1 at L/P = 24, passed through the Sepharose CL-6B column pre-equilibrated with buffer 1 and Q was measured again for each preparation as above.

Differential release of calcein and TRD-40k– POPC/POPS/PEG-PE (1:1:0.02 mole ratio) liposomes co-encapsulated with TRD-40k and calcein were treated with MAX1 at a ratio of L/P =24 for 10 min and then passed through the Sepharose CL-6B column pre-equilibrated with buffer 1. Release of TRD-40k and calcein from the collected fractions was then determined by measuring the fluorescence intensity of Texas red dextran at λ_{ex} = 590 nm and λ_{em} = 615 nm and calcein at λ_{ex} = 490 nm and λ_{em} = 517 nm in a 96 well plate using SpectraMax M2 (Molecular Devices, Sunnyvale, CA).

Atomistic molecular dynamics simulations

We constructed *β*-hairpin barrels/channels with three cation-rich-peptides, MAX1, MAX35, and MAX8V16E, using the CHARMM program (10). These MAX *β*-hairpins have a turn at 10^{D}P-11P, where ^{D}P denotes the D-amino acid proline. In the MD simulations, peptides had free N-termini (-NH_3^+) and amidated C-termini (-NH_2). The MAX barrels/channels were embedded in a lipid bilayer containing POPC and POPS with a mole ratio of 3:1. The cross-section areas per lipid for POPC and POPS are 68.3 Å^2 and 55.0 Å^2, respectively (11,12). With a choice for the number of lipid molecules, the optimal value of lateral cell dimensions can be determined. A unit cell containing two layers of lipids was constructed. A lipid bilayer containing a total of 400 lipids constitutes the unit cell with TIP3P waters, added at both sides with lipid/water ratio of ~1/100. Updated CHARMM all-atom additive force field for lipids (C36) (13) and the modified TIP3P water model (14) were used to construct the set of starting points and to relax the systems to a production-ready stage. Our simulations contain a D-amino acid residue. To simulate the D-amino acid, we adapted the standard L-amino acid parameters using a mirror-image of the dihedral angle cross term map (CMAP) correction (15) by reflecting the phi-psi CMAP matrix (16,17). The barrels/channels-lipid systems have net negative charges. To neutralize the system,

ten (10 Na^+) counterions for both MAX1 and MAX35 systems and forty (40 Na^+) counter ions for the MAX8V16E simulations were added to the bilayer system. In addition, to obtain a salt concentration near 100 mM, an additional 66 Na^+ and 66 Cl^- ions were added to the bilayer systems. The bilayer system containing a MAX barrel/channel, lipids, salts, and waters contained approximately 180,000 atoms.

The MAX barrels/channels within explicit solvents were gradually relaxed with the peptides held rigid. In the pre-equilibrium stages, a series of minimizations and dynamic cycles were performed for the initial systems to remove overlaps of the alkane chains in the lipids and to relax the solvents around the harmonically restrained peptides. The harmonic restraints were gradually diminished with the full Ewald electrostatics calculation and constant temperature (Nosé–Hoover) thermostat/barostat at 303 K. For $t < 30$ ns, our simulation employed the NPAT (constant number of atoms, pressure, surface area, and temperature) ensemble with a constant normal pressure applied in the direction perpendicular to the membrane. After $t = 30$ ns, the simulations employed the NPT ensemble. For production runs to 100 ns for all systems, the NAMD code (18) on a Biowulf cluster at the National Institutes of Health (Bethesda, MD) was used for the starting point. Averages were taken after 30 ns, discarding initial transients.

DOCUMENT S2

Calculation of the number of MAX binding sites per vesicle assuming 9 POPS molecules/binding site to neutralize all the charges on the peptide

For a vesicle with outer diameter d = 110 nm, the vesicle outer area: πd^2 = 38013 nm^2.

The area/lipid = 0.68 nm^2.

The number of lipids in the outer monolayer = Vesicle outer area/Area/lipid = 55902.

For 50% POPS the total number of POPS molecules on the outer surface is 55902/4 = 13976 (Half the lipids are POPS; half are on the outer monolayer which makes a quarter of total lipid).

For 9 POPS molecules/binding site the number of binding sites is 13976/9 = 1553.

Calculation of leakage of vesicle contents through a single pore

The membrane permeability can be expressed by a flux of a substance per unit area of pores, J mol/($m^2 \cdot s^{-1}$), which follows Fick's law,

$$J = -P(C^{in}(t) - C^{out}(t)) = -(D/h)(C^{in}(t) - C^{out}(t)) \quad (1)$$

where P (m/s) is permeability coefficient and $C^{out}(t)$ (mol/m^3) is concentration outside at time t. P is equal to D/h, where D (m^2/s) is diffusion coefficient and h (m) is the effective length of the pore, which is almost the same as the membrane thickness (h = 3.5 nm). Therefore the rate of leakage of the fluorescent probe from a liposome can be expressed as follows (here we assume C^{out} =0 for any time, because the volume of the outside the liposome is very large),

$$V(dC^{in}/dt) = -(D/h)S_pC^{in} \quad (2)$$

where V is the volume of the liposome and S_p is the area of the pore. Therefore,

$$C^{in}(t)/C^{in}(0) = \exp(-k_{leak}t) \quad (3)$$

where $k_{leak} = DS_p/hV$.

Here, $D = 3.3 \times 10^{-10}$ m^2s^{-1}; $S_p = \pi r^2 = 7.06858 \times 10^{-18}$ m^2, where pore radius r = 1.5 nm; $h = 3.5 \times 10^{-9}$ m; and $V = 4\pi R^3/3 = 1.5708 \times 10^{-21}$ m^3, where liposome radius R = 50 nm.

Using these numbers, we obtained that k_{leak} = 424 s^{-1}. Therefore according to equation (3), 50% leaks out in 1.6 ms, 90% in 5.4 ms, and 99% in 10.8 ms.

SUPPORT ING REFERENCES

1. Szoka, F., Jr., and D. Papahadjopoulos. 1980. Comparative properties and methods of preparation of lipid vesicles (liposomes). Annu Rev Biophys Bioeng 9:467-508.
2. Wilschut, J., N. Duzgunes, R. Fraley, and D. Papahadjopoulos. 1980. Studies on the mechanism of membrane fusion: kinetics of calcium ion induced fusion of phosphatidylserine vesicles followed by a new assay for mixing of aqueous vesicle contents. Biochemistry 19:6011-6021.
3. Tamba, Y., H. Ariyama, V. Levadny, and M. Yamazaki. 2010. Kinetic pathway of antimicrobial peptide magainin 2-induced pore formation in lipid membranes. J Phys Chem B 114:12018-12026.
4. Duzgunes, N., J. Wilschut, K. Hong, R. Fraley, C. Perry, D. S. Friend, T. L. James, and D. Papahadjopoulos. 1983. Physicochemical characterization of large unilamellar phospholipid vesicles prepared by reverse-phase evaporation. Biochim Biophys Acta 732:289-299.
5. Ames, B. N., and D. T. Dubin. 1960. The role of polyamines in the neutralization of bacteriophage deoxyribonucleic acid. J Biol Chem 235:769-775.
6. Gupta, K., V. P. Singh, R. K. Kurupati, A. Mann, M. Ganguli, Y. K. Gupta, Y. Singh, K. Saleem, S. Pasha, and S. Maiti. 2009. Nanoparticles of cationic chimeric peptide and sodium polyacrylate exhibit striking antinociception activity at lower dose. J Control Release 134:47-54.
7. Sinthuvanich, C., A. S. Veiga, K. Gupta, D. Gaspar, R. Blumenthal, and J. P. Schneider. 2012. Anticancer beta-hairpin peptides: membrane-induced folding triggers activity. J Am Chem Soc 134:6210-6217.
8. Duzgunes, N., H. Faneca, and M. C. Lima. 2010. Methods to monitor liposome fusion, permeability, and interaction with cells. Methods Mol Biol 606:209-232.
9. Weinstein, J. N., R. D. Klausner, T. Innerarity, E. Ralston, and R. Blumenthal. 1981. Phase transition release, a new approach to the interaction of proteins with lipid vesicles. Application to lipoproteins. Biochim Biophys Acta 647:270-284.
10. Brooks, B. R., R. E. Bruccoleri, B. D. Olafson, D. J. States, S. Swaminathan, and M. Karplus. 1983. Charmm - a program for macromolecular energy, minimization, and dynamics calculations. J. Comp. Chem. 4:187-217.
11. Kucerka, N., S. Tristram-Nagle, and J. F. Nagle. 2005. Structure of fully hydrated fluid phase lipid bilayers with monounsaturated chains. J Membr Biol 208:193-202.
12. Mukhopadhyay, P., L. Monticelli, and D. P. Tieleman. 2004. Molecular dynamics simulation of a palmitoyl-oleoyl phosphatidylserine bilayer with Na+ counterions and NaCl. Biophys J 86:1601-1609.
13. Klauda, J. B., R. M. Venable, J. A. Freites, J. W. O'Connor, D. J. Tobias, C. Mondragon-Ramirez, I. Vorobyov, A. D. MacKerell, Jr., and R. W. Pastor. 2010. Update of the CHARMM all-atom additive force field for lipids: validation on six lipid types. J Phys Chem B 114:7830-7843.
14. Durell, S. R., B. R. Brooks, and A. Bennaim. 1994. Solvent-induced forces between two hydrophilic groups. J. Phys. Chem. 98:2198–2202.
15. Mackerell, A. D., M. Feig, and C. L. Brooks. 2004. Extending the treatment of backbone energetics in protein force fields: Limitations of gas-phase quantum mechanics in

reproducing protein conformational distributions in molecular dynamics simulations. J. Comput. Chem. 25:1400-1415.
16. Connelly, L., H. Jang, F. T. Arce, R. Capone, S. A. Kotler, S. Ramachandran, B. L. Kagan, R. Nussinov, and R. Lal. 2012. Atomic force microscopy and MD simulations reveal pore-like structures of all-D-enantiomer of Alzheimer's β-amyloid peptide: relevance to the ion channel mechanism of AD pathology. J Phys Chem B 116:1728-1735.
17. Capone, R., H. Jang, S. A. Kotler, L. Connelly, F. Teran Arce, S. Ramachandran, B. L. Kagan, R. Nussinov, and R. Lal. 2012. All-D-Enantiomer of β-Amyloid Peptide Forms Ion Channels in Lipid Bilayers. J Chem Theory Comput 8:1143-1152.
18. Phillips, J. C., R. Braun, W. Wang, J. Gumbart, E. Tajkhorshid, E. Villa, C. Chipot, R. D. Skeel, L. Kale, and K. Schulten. 2005. Scalable molecular dynamics with NAMD. J. Comput. Chem. 26:1781-1802.